

Near-IR High-Resolution Imaging Polarimetry of the SU Aur Disk: Clues for Tidal Tails?¹

Jerome de Leon^{1,2}, Michihiro Takami¹, Jennifer L. Karr¹, Jun Hashimoto^{3,4}, Tomoyuki Kudo⁵, Michael Sitko⁶, Satoshi Mayama², Nobuyuki Kusakabe⁴, Eiji Akiyama⁴, Haiyu Baobab Liu¹, Tomonori Usuda⁴, Lyu Abe⁷, Wolfgang Brandner⁸, Timothy D. Brandt⁹, Joseph Carson¹⁰, Thayne Currie⁵, Sebastian E. Egner⁵, Markus Feldt⁸, Katherine Follette¹¹, Carol A. Grady^{12,13}, Miwa Goto¹⁴, Olivier Guyon⁵, Yutaka Hayano⁵, Masahiko Hayashi⁴, Saeko Hayashi⁵, Thomas Henning⁸, Klaus W. Hodapp¹⁵, Miki Ishii⁴, Masanori Iye⁴, Markus Janson¹⁶, Ryo Kandori⁴, Gillian R. Knapp⁹, Masayuki Kuzuhara¹⁷, Jungmi Kwon¹⁸, Taro Matsuo¹⁹, Michael W. McElwain¹³, Shoken Miyama²⁰, Jun-Ichi Morino⁴, Amaya Moro-Martin²¹, Tetsuo Nishimura⁵, Tae-Soo Pyo⁵, Eugene Serabyn²², Takuya Suenaga², Hiroshi Suto⁴, Ryuji Suzuki⁴, Yasuhiro Takahashi^{18,23}, Naruhisa Takato⁵, Hiroshi Terada⁵, Christian Thalmann²⁴, Daigo Tomono⁵, Edwin L. Turner^{9,25}, Makoto Watanabe²⁶, John P. Wisniewski³, Toru Yamada²⁷, Hideki Takami⁵, Motohide Tamura^{4,5,18}

ABSTRACT

We present new high-resolution ($\sim 0''.09$) H -band imaging observations of the circumstellar disk around the T Tauri star SU Aur. Our observations with Subaru-HiCIAO have revealed the presence of scattered light as close as $0''.15$ (~ 20 AU) to the star. Within our image, we identify bright emission associated with a disk with a minimum radius of ~ 90 AU, an inclination of $\sim 35^\circ$ from the plane of the sky, and an approximate P.A. of 15° for the major axis. We find a brightness asymmetry between the northern and southern sides of the disk due to a non-axisymmetric disk structure. We also identify a pair of asymmetric tail structures extending east and west from the disk. The western tail extends at least $2''.5$ (350 AU) from the star, and is probably associated with a reflection nebula previously observed at optical and near-IR wavelengths. The eastern tail extends at least $1''$ (140 AU) at the present signal-to-noise. These tails are likely due to an encounter with an unseen brown dwarf, but our results do not exclude the explanation that these tails are outflow cavities or jets.

Subject headings: protoplanetary disks — stars: individual (SU Aur) — stars: pre-main sequence — polarization

¹Institute of Astronomy and Astrophysics, Academia Sinica, P.O. Box 23-141, Taipei 10617, Taiwan, R.O.C.; jpdleon.bsap@gmail.com

²The Center for the Promotion of Integrated Sciences, The Graduate University for Advanced Studies (SO-KENDAI), Shonan International Village, Hayama-cho, Miura-gun, Kanagawa 240-0193, Japan

³H.L. Dodge Department of Physics and Astronomy, University of Oklahoma, 440 W Brooks St Norman, OK 73019, USA

⁴National Astronomical Observatory of Japan, 2-21-1

Osawa, Mitaka, Tokyo 181-8588, Japan

⁵Subaru Telescope, 650 North A'ohoku Place, Hilo, HI 96720, USA

⁶Department of Physics, University of Cincinnati, Cincinnati OH 45221, USA

⁷Laboratoire Lagrange (UMR 7293), Université de Nice-Sophia Antipolis, CNRS, Observatoire de la Côte d'Azur, 28 avenue Valrose, 06108 Nice Cedex 2, France

⁸Max Planck Institute for Astronomy, Königstuhl 17, D-69117 Heidelberg, Germany

⁹Department of Astrophysical Sciences, Princeton Uni-

1. INTRODUCTION

Direct images of scattered light from protoplanetary disks provide valuable information about their surface geometries. Advances in instrumentation have produced high angular resolution, high sensitivity observations, revealing a variety of substructures in protoplanetary disks associated with pre-main sequence (PMS) stars. In particular, near-infrared (IR) imaging polarimetry with adaptive optics has been used extensively during the Strategic Explorations of Exoplanets and

versity, Peyton Hall, Ivy Lane, Princeton, NJ 08544, USA

¹⁰Department of Physics and Astronomy, College of Charleston, 58 Coming St., Charleston, SC 29424, USA

¹¹Kavli Institute of Particle Astrophysics and Cosmology, Stanford University, 452 Lomita Mall, Stanford, CA 94305, USA.

¹²Eureka Scientific, 2452 Delmer Suite 100, Oakland CA 96402, USA

¹³ExoPlanets and Stellar Astrophysics Laboratory, Code 667, Goddard Space Flight Center, Greenbelt, MD 20771, USA

¹⁴Universitäts-Sternwarte München, Scheinerstr. 1, D-81679 Munich, Germany

¹⁵Institute for Astronomy, University of Hawaii, 640 North A'ohoku Place, Hilo, HI 96720, USA

¹⁶Department of Astronomy, Stockholm University, 106 91, Stockholm, Sweden

¹⁷Department of Earth and Planetary Sciences, Tokyo Institute of Technology, 2-12-1 Ookayama, Meguro-ku, Tokyo 152-8551, Japan

¹⁸Department of Astronomy, The University of Tokyo, 7-3-1 Hongo, Bunkyo-ku, Tokyo 113-0033, Japan

¹⁹Department of Astronomy, Kyoto University, Kitashirakawa-Oiwake-cho, Sakyo-ku, Kyoto, Kyoto 606-8502, Japan

²⁰Hiroshima University, 1-3-2 Kagamiyama, Higashi-Hiroshima, 739-8511, Japan

²¹Department of Astrophysics, CAB-CSIC/INTA, 28850 Torrejon de Ardoz, Madrid, Spain

²²Jet Propulsion Laboratory, California Institute of Technology, Pasadena, CA, 91109, USA

²³MEXT, 3-2-2 Kasumigaseki, Chiyoda, Tokyo 100-8959

²⁴Institute for Astronomy, ETH Zurich, Wolfgang-Pauli-Strasse 27, 8093, Zurich, Switzerland

²⁵Kavli Institute for the Physics and Mathematics of the Universe, The University of Tokyo, Kashiwa 277-8568, Japan

²⁶Department of CosmoSciences, Hokkaido University, Kita-ku, Sapporo, Hokkaido 060-0810, Japan

²⁷Astronomical Institute, Tohoku University, Aoba-ku, Sendai, Miyagi 980-8578, Japan

¹Based on data collected at Subaru Telescope, which is operated by the National Astronomical Observatory of Japan.

Disks with Subaru (SEEDS) survey with HiCIAO (Tamura 2009). This survey has been successful in observing diverse disk morphologies, from uniform (e.g., MWC 480—Kusakabe et al. 2012) to complex, including spirals (e.g., AB Aur, SAO 206262, MWC 758—Hashimoto et al. 2011; Muto et al. 2012; Grady et al. 2013), gaps or rings (e.g., PDS 70, 2MASS J1604, Oph IRS 48—Hashimoto et al. 2012; Mayama et al. 2012; Follette et al. 2015), and other asymmetric flux distributions (e.g., UX Tau A, SR 21, RY Tau, Oph IRS 48—Tanii et al. 2012; Follette et al. 2013; Takami et al. 2013; Follette et al. 2015). Some of these structures may be due to dynamical disk-planet interactions providing hints of ongoing planet formation (e.g., Hashimoto et al. 2011, 2012; Muto et al. 2012; Mayama et al. 2012; Grady et al. 2013).

SU Aur is a classical T Tauri star located in the Taurus-Auriga star formation region at a distance of ~ 140 pc (Bertout and Genova 2006). This star-disk system shows large IR and UV excesses indicating the existence of a circumstellar disk and ongoing active mass accretion, respectively (e.g., Bertout et al. 1988; Calvet et al. 2004; Jeffers et al. 2014). Table 1 summarizes its stellar and disk properties.

SU Aur is also associated with a bright reflection nebula (Nakajima and Golimowski 1995; Grady et al. 2001; Chakraborty and Ge 2004; Jeffers et al. 2014). Nakajima and Golimowski (1995) revealed an associated cometary nebulosity at optical wavelengths, extending to the west and southwest at small ($<10''$) and large distances ($10''$ - $30''$), respectively. Optical high-resolution observations using coronagraphy or imaging polarimetry (Grady et al. 2001; Chakraborty and Ge 2004; Jeffers et al. 2014) have resolved the extended nebulosity toward the west within $5''$ of the star. Possible origins of the observed structure include an outflow cavity (Grady et al. 2001; Chakraborty and Ge 2004), part of the circumstellar disk (Chakraborty and Ge 2004), or part of a remnant envelope or parent cloud (Jeffers et al. 2014). Chakraborty and Ge (2004) also applied point-spread function (PSF) subtraction to seeing-limited near-IR images, and report the presence of an extended nebulosity to the southwest, close to the star.

In this paper, we present near-IR imaging polarimetry of SU Aur. Using Subaru-HiCIAO, we

have revealed scattered light from the disk, as well as two tails which may be due to tidal interaction with an unseen brown dwarf. The rest of the paper is organized as follows. In section 2, we summarize our observations and data reduction. In section 3, we show the observed Polarized Intensity (PI) flux distribution and polarization. We highlight the discovery of salient features including the disk and tail structures. In section 4, we discuss the orientation of the disk and the nature of the tail structure.

2. OBSERVATIONS AND DATA REDUCTION

SU Aur was observed in H -band ($1.65 \mu\text{m}$) on 2014 January 19 UT using the high-contrast imager HiCIAO. The adaptive optics system (AO188) provided a stable stellar PSF (FWHM = $0''.08$, Strehl ratio = 0.2–0.3). We used a combination of polarimetric and angular differential imaging (PDI+ADI) modes. A dual Wollaston prism was used to split incident light into two image pairs that are orthogonally and linearly polarized, each with a $5'' \times 5''$ field of view and a pixel scale of $9.5 \text{ mas pixel}^{-1}$. As for several other SEEDS observations, linear polarization was measured by rotating the half-wave plate to four angular positions: 0° , 22.5° , 45° , and 67.5° . We obtained 12 full waveplate cycles, taking a 30-sec exposure per waveplate position, using a 10% neutral density (ND) filter. No coronagraphic mask was used in order to image the innermost region around the central star. Four additional sets of waveplate cycles were obtained using a 1% ND filter to measure the PSF FWHM and the total Stokes I flux density of the star (I_*).

The data were reduced using the standard method for ADI+PDI (Hinkley et al. 2009). The measured Stokes I , Q , and U parameters were used to compute the more accurate intrinsic Stokes parameters. We then calculated the polarized intensity ($\text{PI} = \sqrt{(Q^2 + U^2)}$), polarization (PI/I) and the angle of polarization ($\theta_P = 0.5 \times \arctan(U/Q)$). The instrumental polarization of HiCIAO at the Nasmyth platform was corrected following Joos et al. (2008) with errors of $<0.1\%$.

To increase the signal-to-noise, we convolved the Q and U images with a Gaussian having a FWHM of $0''.04$. As a result, the angular resolu-

tion of the images shown in later sections is $0''.09$, slightly larger than the instrumental resolution.

We also applied the LOCI algorithm (Lafrenière et al. 2007) to the Stokes I images to search for faint companions, with parameters as in Table 2. The image rotation during the observations was small ($\sim 8^\circ$) hence we needed a small N_σ (the minimum displacement distance in the azimuthal direction) to search for a companion close to the star (down to $r=0''.17$ and $0''.36$ for $N_\sigma=0.1$ and $0.5 \times \text{FWHM}$ of the observations, respectively). The other LOCI parameters were the same for the four sets and were standard and optimum for SEEDS observations. We embedded artificial point sources at different radii and derived upper limits for $3\text{-}\sigma$ fluxes of the companion of $m_H \sim 15$, ~ 19 , 21.0 and 21.5 at $r=0''.16$, $0''.5$, $1''$, and $2''$ from the star, respectively. The detection limits were almost identical between different parameter sets.

3. RESULTS

Figure 1 shows the observed PI flux distribution overlaid with polarization vectors. There is bright emission at the center with a radius of ~ 100 AU. This emission probably originated from a protoplanetary disk elongated to the north-south, slightly offset in the counter-clockwise direction. The peak emission in the disk is located at $r \sim 0''.20$ (~ 28 AU) north of the star and has PI/I_* of $2.9 \times 10^{-6} \text{ pix}^{-1}$. This translates to surface brightness in PI of $\sim 80 \text{ mJy arcsec}^{-2}$. This is comparable to the brightest disks in the SEEDS observations summarized in Takami et al. (2014). Moreover, the distribution shows a deficit of emission perpendicular to the semi-major axis similar to PI distributions observed in other disks with intermediate inclination angles (e.g., Hashimoto et al. 2012; Kusakabe et al. 2012; Tanii et al. 2012). This deficit likely arises because along the minor axis, the light is dominated by forward- and backward-scattered photons, which are intrinsically less polarized (e.g., Takami et al. 2013), and does not require an actual deficit of material in the disk. We detect a brightness asymmetry between the disk's northern and southern sides: the northern side is brighter than the southern side by a factor of 2.

To analyze the inclination and orientation of SU Aur's disk, we fit an ellipse to the outermost contour ($\text{PI}/I_* = 10^{-7} \text{ pix}^{-1}$) by a simple visual

analysis. This fit yields angular separations of $1''.7$ and $1''.4$ (~ 240 AU and ~ 200 AU) for the major and minor axes, respectively, with a position angle (P.A.) of $\sim 15^\circ$ for the major axis. The ratio between the minor and major axes indicates an approximate disk inclination of 35° . We do not make a more quantitative or accurate measurement for the disk orientation or inclination because of the asymmetric geometry seen in the contour.

We extracted the radial PI/I_* profiles wherein we averaged a swath of 11 pixels ($\sim 0''.1$) along the disk's major axis on both sides of the star. A power-law function was fitted to each profile, as shown in Figure 2. Between $0''.25$ and $0''.6$, we find the following power-law indices that best fit the observed PI profiles: ~ -3 and ~ -2 at P.A. of 15° and 195° , respectively. The indices we measured are roughly consistent with SEEDS studies of several disks (SAO 206462, MWC 480, MWC 758 — Muto et al. 2012; Kusakabe et al. 2012; Grady et al. 2013) as well as some other observations of disks associated with Herbig Ae and Be stars (Fukagawa et al. 2010). Compared with P.A. = 15° , the observed profile shows a larger deviation from the power-law fit at P.A. = 195° (i.e., shallower and steeper slopes at inner and outer radii, respectively). A different brightness distribution between these two P.A.s indicates that the disk structure is non-axisymmetric.

Figure 2 also shows a drop-off in the observed flux at $0''.6$ – $0''.7$ from the star. This indicates a lower limit for the disk radius of ~ 90 AU at a distance of 140 pc. This is consistent with disk models for millimeter emission and optical-to-millimeter spectral energy distributions by Ricci et al. (2010) (100–300 AU) and Jeffers et al. (2014) (500 AU), respectively. Note that the absence of flux in the outer region does not imply the absence of disk material as it may be due to self-shadowing of the disk (Takami et al. 2014).

In Figure 1, a long, faint tail ($PI/I_* \lesssim 0.5 \times 10^{-7}$ or 1.4 mJy arcsec $^{-2}$) extending westward at least $2''.5$ (350 AU) can also be seen. We also find an extended component that is marginally detected from the north-east to the east side of the disk. The tail in the west is likely associated with the extended reflection nebula previously observed at optical and near-IR wavelengths (Nakajima and Golimowski 1995; Grady et al. 2001; Chakraborty and Ge 2004; Jeffers et al. 2014). However, the

distribution of emission appears significantly narrower in the north-south direction than previous observations in the optical and near-IR.

To better display structures in the faint outer regions, we convolve the PI image with a Gaussian of $FWHM=0''.1$ and then scale the PI flux at each pixel by R^2 , where R is the projected distance from the star (Figure 3). The figure clearly shows two tails extending east and west. In Figure 3, the tails appear to be associated with the edge of the disk emission, however, observations with higher signal-to-noise are required to confirm this.

Figure 1 also shows the polarization vector map. The vectors in the disk show a centrosymmetric pattern, as has been observed in several other disks with near-IR imaging polarimetry (e.g., Hashimoto et al. 2011). This indicates that the disk is seen in scattered light that originated from the central star. Similarly, the vectors in the tail indicate that it is illuminated by the star-disk system. The disk has lower fractional polarization ($\lesssim 10\%$) than the western tail (up to $\sim 30\%$). This is because the Stokes I flux within $1''$ of the star is dominated by the star's PSF halo, lowering the degree of polarization (PI/I). Hence, the vectors represent the lower limit of the true degree of polarization.

4. DISCUSSION

Jeffers et al. (2014) conducted optical imaging polarimetry of SU Aur and found a disk-like morphology elongated in the east-west direction at a larger angular scale (radius of $\sim 2''$). The disk-like structure within $1''$ of the star seen in the near-IR (Figure 1) is almost perpendicular to this structure in the optical. As the dust opacity is higher in the optical than in the near-IR, the disk may be partially obscured by dust in the envelope at optical wavelengths. Thus, near-IR observations should have an advantage in observing scattered light close to the disk surface (Fukagawa et al. 2004). This explanation is supported by the fact that the power-law indices of the radial PI distribution in the near-IR are similar to other disk systems (Section 3).

Tails like those in Figures 1 and 3 are not usually observed in scattered light associated with young stellar objects (YSOs). An exception may be a jet-like feature in the Z CMa system observed

by Millan-Gabet and Monnier (2002), which the authors attributed to a cavity wall. In the remaining section we discuss possible origins of these tails: (1) outflow cavities, (2) collimated jets, and (3) tidal tails due to a (sub-)stellar encounter.

Before discussing the nature of the SU Aur tails in detail, we estimate the dust mass of the western tail. Takami et al. (2013) derived the following equation to estimate the dust mass observed in scattered light using imaging polarimetry:

$$m_{dust} = \int \frac{n_{PI}(\mathbf{r})}{n_*} \frac{r^2}{\kappa_{ext}} \left(\frac{PI}{I_0} \right)^{-1} d\mathbf{r} \quad (1)$$

where m_{dust} is the dust mass; $n_{PI}(\mathbf{r})$ is the number of PI photons at each position; n_* is the number of stellar I photons; r is the distance to the star; κ_{ext} is the dust opacity; PI/I_0 is the fraction of the PI flux normalized to the incident flux on the dust grains. Here we assume the interstellar dust size distribution measured by Kim et al. (1994). This yields $\kappa_{ext} = 5.3 \times 10^3 \text{ cm}^2 \text{ g}^{-1}$ and $PI/I_0 \sim 0.01$ at a wavelength of $1.65 \mu\text{m}$ (Takami et al. 2013). Integrating Equation (1) from disk edge to the tail end in Figure 1 ($\sim 110 - 350 \text{ AU}$) yields a dust mass of $\sim 6 \times 10^{-8} M_\odot$, if we use the projected distance for r at the distance of 140 pc. This mass is smaller than the disk’s dust mass inferred from millimeter interferometry (see Table 1) by a factor of 2000–5000. However, like protoplanetary disks, a significantly larger mass might exist behind the scattering layer. The above dust mass should therefore be a lower limit for the tail.

SU Aur is known to be associated with a reflection nebula in the east-west direction, approximately the same direction as the tails in Figures 1 and 3, and to the southwest at larger angular scales (Nakajima and Golimowski 1995; Grady et al. 2001; Chakraborty and Ge 2004; Jeffers et al. 2014). Such nebulosity associated with YSOs is often attributed to an outflow cavity (e.g., Tamura et al. 1991; Hodapp 1994; Lucas and Roche 1998; Padgett et al. 1999). However, this explanation may not apply to these tails for several reasons. First, the tails shown in Figures 1 and 3 are significantly narrower than other YSO outflow cavities, which generally have a wide opening angle. Secondly, an outflow cavity in scattered light is usually observed toward a single direction unless we see the disk edge-on (e.g., Fischer et al. 1994; Whitney et al. 2003). However, the tails in Fig-

ures 1 and 3 are seen in two opposite directions despite the fact that the disk has an intermediate viewing angle.

Another possible explanation for the tails may be that these are collimated jets. Many YSOs are associated with such jets (e.g., Frank et al. 2014, for a review), however, these are not usually observed in scattered light. To further investigate this explanation, we estimate the mass ejection rate and compare it with the disk accretion rate. Using Equation (1) we derive a dust mass of $3 \times 10^{23} \text{ g AU}^{-1}$ along the western tail at 200 AU from the star. This would yield a mass ejection rate of $2 \times 10^{-7} M_\odot \text{ yr}^{-1}$, assuming a typical jet velocity of 50 km s^{-1} (e.g., Hartigan et al. 1995; Hirth et al. 1997) and gas-to-dust mass ratio of 100. This is 7–40 times larger than the disk accretion rate measured by Calvet et al. (2004) and Ricci et al. (2010) (see Table 1). The mass ejection to mass accretion ratio would be even larger if the tail contains more gas and dust than is inferred from the scattered light. However, such a high mass ejection to mass accretion ratio is not feasible for PMS stars, which usually show a mass ejection to mass accretion ratio of ~ 0.1 (e.g., Calvet 1997). Therefore, jets are not likely to explain the tail structure either, unless the jet velocity is significantly lower (e.g., $\lesssim 10 \text{ km s}^{-1}$) than for other similar objects.

Tidal interaction with a star or a brown dwarf may alternatively explain the observed tail structures. Kinematic simulations of stellar encounters show that this physical process produces tails similar to those in Figures 1 and 3 (e.g. Pfalzner 2003; Forgan and Rice 2009). A tidal tail was observed in the RW Aur disk system using millimeter interferometry (Cabrit et al. 2006). A difficulty with this interpretation is that there is yet no observational evidence of another star within $30''$ of SU Aur (Nakajima and Golimowski 1995; Grady et al. 2001; Chakraborty and Ge 2004; Jeffers et al. 2014, see also data archive for 2MASS). However, an encounter with an unseen brown dwarf (BD) could produce tails observable in scattered light. We estimate an upper limit BD mass of $0.6-2 \times 10^{-3} M_\odot$ for our field of view of observations with a detection limit of 21.0–21.5 mag (Section 2) and the COND models for 1–10 Myr (Baraffe et al. 2003). The same models and the completeness limit of the 2MASS Point Source Catalog (15.1 mag) yield an

upper limit mass of $0.8\text{-}2 \times 10^{-2} M_{\odot}$.

A (sub-)stellar encounter would affect the disk structure, and therefore affect mass accretion and planet formation (e.g. Pfalzner 2003; Forgan and Rice 2009, 2010; Breslau et al. 2014). SU Aur would be a good, rare observational example to test these theories in detail. Confirmation of this physical process in this system would require deep imaging to search for a nearby brown dwarf, and kinematic information for the disk and the tail from millimeter interferometry. A search for jet emission at optical and near-IR wavelengths would also be a good test for the jet hypothesis (Frank et al. 2014).

5. CONCLUSIONS

We present *H*-band imaging polarimetry of scattered light from the circumstellar disk around the T Tauri star SU Aur. Our high-resolution ($0''.09$) image of polarized intensity has allowed us to observe scattered light from the disk as close as $0''.15$ (~ 20 AU) to the star. We identify bright emission probably associated with the disk, elongated along an approximate P.A. of 15° . From its distribution, we estimate a minimum disk radius of ~ 90 AU and a disk inclination of $\sim 35^{\circ}$. As observed in several protoplanetary disks, the surface brightness along the disk's major axis is approximately proportional to r^{-2} to r^{-3} at $r=0''.2\text{-}0''.65$, where r is the projected distance to the star. The brightness distribution of the scattered light is asymmetric between the disk's northern and southern sides indicating a non-axisymmetric disk structure.

Our near-IR images also show two tails extending to the east and west of the disk. The western tail extends at least $2''.5$ (350 AU) from the star, and is probably associated with an extended reflection nebula previously observed at optical and near-IR wavelengths. The eastern tail extends at least $1''$ (140 AU) at the present signal-to-noise. We estimate a lower limit of the dust mass of the western tail ($r=110\text{-}350$ AU) of $\sim 6 \times 10^{-8} M_{\odot}$ using an interstellar dust model and assuming that the tail lies close to the plane of the sky. This mass is significantly lower than the disk's dust mass inferred from millimeter interferometry ($1 - 3 \times 10^{-4} M_{\odot}$).

Possible explanations for the tails include (1)

outflow cavities, (2) collimated jets, and (3) tidal interaction with a brown dwarf. The morphology and brightness favor the last explanation, but these do not rule out the other possibilities. Confirmation requires searching for a nearby brown dwarf with deep imaging, and observing the kinematics of the disk and tails using millimeter interferometry.

We thank the Subaru Telescope staff for their support, especially Michael Lemmen for making our observations successful. We also thank Drs. Kazushi Sakamoto, Shigehisa Takakuwa, Lihwai Lin, Yoichi Ohyama, Pin-Gao Gu and Henry Hsieh for useful discussions. M.T. is supported from Ministry of Science and Technology (MoST) of Taiwan (Grant No. 103-2112-M-001-029). C.A.G. acknowledges support under NSF AST 1008440. This research made use of the Simbad database operated at CDS, Strasbourg, France, and the NASA's Astrophysics Data System Abstract Service.

Facilities: Subaru (HiCIAO).

REFERENCES

- Baraffe, I., Chabrier, G., Barman, T.S., Allard, F., and Hauschildt, P.H.: 2003, *A&A* **402**, 701
- Bertout, C., Basri, G., and Bouvier, J.: 1988, *ApJ* **330**, 350
- Bertout, C. and Genova, F.: 2006, *A&A* **460**, 499
- Bertout, C., Siess, L., and Cabrit, S.: 2007, *A&A* **473**, L21
- Breslau, A., Steinhausen, M., Vincke, K., and Pfalzner, S.: 2014, *A&A* **565**, A130
- Cabrit, S., Pety, J., Pesenti, N., and Dougados, C.: 2006, *A&A* **452**, 897
- Calvet, N.: 1997, in B. Reipurth and C. Bertout (eds.), *Herbig-Haro Flows and the Birth of Stars*, Vol. 182 of *IAU Symposium*, pp 417-432
- Calvet, N., Muzerolle, J., Briceño, C., Hernández, J., Hartmann, L., Saucedo, J. L., and Gordon, K. D.: 2004, *AJ* **128**, 1294
- Chakraborty, A. and Ge, J.: 2004, *AJ* **127**, 2898

- Fischer, O., Henning, T., and Yorke, H. W.: 1994, *A&A* **284**, 187
- Follette, K. B., Grady, C. A., Swearingen, J. R., Sitko, M. L., Champney, E. H., van der Marel, N., Takami, M., Kuchner, M. J., Close, L. M., Muto, T., Mayama, S., McElwain, M. W., Fukagawa, M., Maaskant, K., Min, M., Russell, R. W., Kudo, T., Kusakabe, N., Hashimoto, J., Abe, L., Akiyama, E., Brandner, W., Brandt, T. D., Carson, J., Currie, T., Egner, S. E., Feldt, M., Goto, M., Guyon, O., Hayano, Y., Hayashi, M., Hayashi, S., Henning, T., Hodapp, K., Ishii, M., Iye, M., Janson, M., Kandori, R., Knapp, G. R., Kuzuhara, M., Kwon, J., Matsuo, T., Miyama, S., Morino, J.-I., Moro-Martin, A., Nishimura, T., Pyo, T.-S., Serabyn, E., Suenaga, T., Suto, H., Suzuki, R., Takahashi, Y., Takato, N., Terada, H., Thalmann, C., Tomono, D., Turner, E. L., Watanabe, M., Wisniewski, J. P., Yamada, T., Takami, H., Usuda, T., and Tamura, M.: 2015, *ApJ* **798**, 132
- Follette, K. B., Tamura, M., Hashimoto, J., Whitney, B., Grady, C., Close, L., Andrews, S. M., Kwon, J., Wisniewski, J., Brandt, T. D., Mayama, S., Kandori, R., Dong, R., Abe, L., Brandner, W., Carson, J., Currie, T., Egner, S. E., Feldt, M., Goto, M., Guyon, O., Hayano, Y., Hayashi, M., Hayashi, S., Henning, T., Hodapp, K., Ishii, M., Iye, M., Janson, M., Knapp, G. R., Kudo, T., Kusakabe, N., Kuzuhara, M., McElwain, M. W., Matsuo, T., Miyama, S., Morino, J.-I., Moro-Martin, A., Nishimura, T., Pyo, T.-S., Serabyn, E., Suto, H., Suzuki, R., Takami, M., Takato, N., Terada, H., Thalmann, C., Tomono, D., Turner, E. L., Watanabe, M., Yamada, T., Takami, H., and Usuda, T.: 2013, *ApJ* **767**, 10
- Forgan, D. and Rice, K.: 2009, *MNRAS* **400**, 2022
- Forgan, D. and Rice, K.: 2010, *MNRAS* **402**, 1349
- Frank, A., Ray, T. P., Cabrit, S., Hartigan, P., Arce, H. G., Bacciotti, F., Bally, J., Benisty, M., Eisloffel, J., Güdel, M., Lebedev, S., Nisini, B., and Raga, A.: 2014, *Protostars and Planets VI* pp 451–474
- Fukagawa, M., Hayashi, M., Tamura, M., Itoh, Y., Hayashi, S. S., Oasa, Y., Takeuchi, T., Morino, J.-i., Murakawa, K., Oya, S., Yamashita, T., Suto, H., Mayama, S., Naoi, T., Ishii, M., Pyo, T.-S., Nishikawa, T., Takato, N., Usuda, T., Ando, H., Iye, M., Miyama, S. M., and Kaifu, N.: 2004, *ApJ* **605**, L53
- Fukagawa, M., Tamura, M., Itoh, Y., Oasa, Y., Kudo, T., Hayashi, S. S., Kato, E., Ootsubo, T., Itoh, Y., Shibai, H., and Hayashi, M.: 2010, *PASJ* **62**, 347
- Grady, C., Stapelfeldt, K., Clampin, M., Padgett, D., Woodgate, B., Henning, T., Grinin, V., Quirrenbach, A., Stecklum, B., Sitko, M., and Biggs, J.: 2001, in *American Astronomical Society Meeting Abstracts*, Vol. 33 of *Bulletin of the American Astronomical Society*, p. 1396
- Grady, C. A., Muto, T., Hashimoto, J., Fukagawa, M., Currie, T., Biller, B., Thalmann, C., Sitko, M. L., Russell, R., Wisniewski, J., Dong, R., Kwon, J., Sai, S., Hornbeck, J., Schneider, G., Hines, D., Moro Martín, A., Feldt, M., Henning, T., Pott, J.-U., Bonnefoy, M., Bouwman, J., Lacour, S., Mueller, A., Juhász, A., Crida, A., Chauvin, G., Andrews, S., Wilner, D., Kraus, A., Dahm, S., Robitaille, T., Jang-Condell, H., Abe, L., Akiyama, E., Brandner, W., Brandt, T., Carson, J., Egner, S., Follette, K. B., Goto, M., Guyon, O., Hayano, Y., Hayashi, M., Hayashi, S., Hodapp, K., Ishii, M., Iye, M., Janson, M., Kandori, R., Knapp, G., Kudo, T., Kusakabe, N., Kuzuhara, M., Mayama, S., McElwain, M., Matsuo, T., Miyama, S., Morino, J.-I., Nishimura, T., Pyo, T.-S., Serabyn, G., Suto, H., Suzuki, R., Takami, M., Takato, N., Terada, H., Tomono, D., Turner, E., Watanabe, M., Yamada, T., Takami, H., Usuda, T., and Tamura, M.: 2013, *ApJ* **762**, 48
- Hartigan, P., Edwards, S., and Ghandour, L.: 1995, *ApJ* **452**, 736
- Hashimoto, J., Tamura, M., Muto, T., Kudo, T., Fukagawa, M., Fukue, T., Goto, M., Grady, C. A., Henning, T., Hodapp, K., Honda, M., Inutsuka, S., Kokubo, E., Knapp, G., McElwain, M. W., Momose, M., Ohashi, N., Okamoto, Y. K., Takami, M., Turner, E. L., Wisniewski, J., Janson, M., Abe, L., Brandner, W., Carson, J., Egner, S., Feldt, M., Golota, T., Guyon,

- O., Hayano, Y., Hayashi, M., Hayashi, S., Ishii, M., Kandori, R., Kusakabe, N., Matsuo, T., Mayama, S., Miyama, S., Morino, J.-I., Moro-Martin, A., Nishimura, T., Pyo, T.-S., Suto, H., Suzuki, R., Takato, N., Terada, H., Thalmann, C., Tomono, D., Watanabe, M., Yamada, T., Takami, H., and Usuda, T.: 2011, *ApJ* **729**, L17
- Hashimoto, J., Dong, R., Kudo, T., Honda, M., McClure, M. K., Zhu, Z., Muto, T., Wisniewski, J., Abe, L., Brandner, W., Brandt, T., Carson, J., Egner, S., Feldt, M., Fukagawa, M., Goto, M., Grady, C. A., Guyon, O., Hayano, Y., Hayashi, M., Hayashi, S., Henning, T., Hodapp, K., Ishii, M., Iye, M., Janson, M., Kandori, R., Knapp, G., Kusakabe, N., Kuzuhara, M., Kwon, J., Matsuo, T., Mayama, S., McElwain, M. W., Miyama, S., Morino, J.-I., Moro-Martin, A., Nishimura, T., Pyo, T.-S., Serabyn, G., Suenaga, T., Suto, H., Suzuki, R., Takahashi, Y., Takami, M., Takato, N., Terada, H., Thalmann, C., Tomono, D., Turner, E. L., Watanabe, M., Yamada, T., Takami, H., Usuda, T., and Tamura, M.: 2012, *ApJ* **758**, L19
- Herbig, G. H.: 1952, *JRASC* **46**, 222
- Hinkley, S., Oppenheimer, B. R., Soummer, R., Brenner, D., Graham, J. R., Perrin, M. D., Sivaramakrishnan, A., Lloyd, J. P., Roberts, Jr., L. C., and Kuhn, J.: 2009, *ApJ* **701**, 804
- Hirth, G. A., Mundt, R., and Solf, J.: 1997, *A&AS* **126**, 437
- Hodapp, K.-W.: 1994, *ApJS* **94**, 615
- Jeffers, S. V., Min, M., Canovas, H., Rodenhuis, M., and Keller, C. U.: 2014, *A&A* **561**, A23
- Joos, F., Buenzli, E., Schmid, H. M., and Thalmann, C.: 2008, in *Society of Photo-Optical Instrumentation Engineers (SPIE) Conference Series*, Vol. 7016 of *Society of Photo-Optical Instrumentation Engineers (SPIE) Conference Series*, p. 48
- Kim, S., Martin, P. G., and Hendry, P. D.: 1994, *ApJ* **422**, 164
- Kusakabe, N., Grady, C. A., Sitko, M. L., Hashimoto, J., Kudo, T., Fukagawa, M., Muto, T., Wisniewski, J. P., Min, M., Mayama, S., Werren, C., Day, A. N., Beerman, L. C., Lynch, D. K., Russell, R. W., Brafford, S. M., Kuzuhara, M., Brandt, T. D., Abe, L., Brandner, W., Carson, J., Egner, S., Feldt, M., Goto, M., Guyon, O., Hayano, Y., Hayashi, M., Hayashi, S. S., Henning, T., Hodapp, K. W., Ishii, M., Iye, M., Janson, M., Kandori, R., Knapp, G. R., Matsuo, T., McElwain, M. W., Miyama, S., Morino, J.-I., Moro-Martin, A., Nishimura, T., Pyo, T.-S., Suto, H., Suzuki, R., Takami, M., Takato, N., Terada, H., Thalmann, C., Tomono, D., Turner, E. L., Watanabe, M., Yamada, T., Takami, H., Usuda, T., and Tamura, M.: 2012, *ApJ* **753**, 153
- Lafrenière, D., Marois, C., Doyon, R., Nadeau, D., and Artigau, É.: 2007, *ApJ* **660**, 770
- Lucas, P. W. and Roche, P. F.: 1998, *MNRAS* **299**, 699
- Mayama, S., Hashimoto, J., Muto, T., Tsukagoshi, T., Kusakabe, N., Kuzuhara, M., Takahashi, Y., Kudo, T., Dong, R., Fukagawa, M., Takami, M., Momose, M., Wisniewski, J. P., Follette, K., Abe, L., Akiyama, E., Brandner, W., Brandt, T., Carson, J., Egner, S., Feldt, M., Goto, M., Grady, C. A., Guyon, O., Hayano, Y., Hayashi, M., Hayashi, S., Henning, T., Hodapp, K. W., Ishii, M., Iye, M., Janson, M., Kandori, R., Kwon, J., Knapp, G. R., Matsuo, T., McElwain, M. W., Miyama, S., Morino, J.-I., Moro-Martin, A., Nishimura, T., Pyo, T.-S., Serabyn, E., Suto, H., Suzuki, R., Takato, N., Terada, H., Thalmann, C., Tomono, D., Turner, E. L., Watanabe, M., Yamada, T., Takami, H., Usuda, T., and Tamura, M.: 2012, *ApJ* **760**, L26
- Millan-Gabet, R. and Monnier, J. D.: 2002, *ApJ* **580**, L167
- Muto, T., Grady, C. A., Hashimoto, J., Fukagawa, M., Hornbeck, J. B., Sitko, M., Russell, R., Werren, C., Curé, M., Currie, T., Ohashi, N., Okamoto, Y., Momose, M., Honda, M., Inutsuka, S., Takeuchi, T., Dong, R., Abe, L., Brandner, W., Brandt, T., Carson, J., Egner, S., Feldt, M., Fukue, T., Goto, M., Guyon, O., Hayano, Y., Hayashi, M., Hayashi, S., Henning, T., Hodapp, K. W., Ishii, M., Iye, M.,

- Janson, M., Kandori, R., Knapp, G. R., Kudo, T., Kusakabe, N., Kuzuhara, M., Matsuo, T., Mayama, S., McElwain, M. W., Miyama, S., Morino, J.-I., Moro-Martin, A., Nishimura, T., Pyo, T.-S., Serabyn, E., Suto, H., Suzuki, R., Takami, M., Takato, N., Terada, H., Thalmann, C., Tomono, D., Turner, E. L., Watanabe, M., Wisniewski, J. P., Yamada, T., Takami, H., Usuda, T., and Tamura, M.: 2012, *ApJ* **748**, L22
- Nakajima, T. and Golimowski, D. A.: 1995, *AJ* **109**, 1181
- Padgett, D. L., Brandner, W., Stapelfeldt, K. R., Strom, S. E., Terebey, S., and Koerner, D.: 1999, *AJ* **117**, 1490
- Pfalzner, S.: 2003, *ApJ* **592**, 986
- Ricci, L., Testi, L., Natta, A., Neri, R., Cabrit, S., and Herczeg, G. J.: 2010, *A&A* **512**, A15
- Takami, M., Karr, J. L., Hashimoto, J., Kim, H., Wisniewski, J., Henning, T., Grady, C. A., Kandori, R., Hodapp, K. W., Kudo, T., Kusakabe, N., Chou, M.-Y., Itoh, Y., Momose, M., Mayama, S., Currie, T., Follette, K. B., Kwon, J., Abe, L., Brandner, W., Brandt, T. D., Carson, J., Egner, S. E., Feldt, M., Guyon, O., Hayano, Y., Hayashi, M., Hayashi, S., Ishii, M., Iye, M., Janson, M., Knapp, G. R., Kuzuhara, M., McElwain, M. W., Matsuo, T., Miyama, S., Morino, J.-I., Moro-Martin, A., Nishimura, T., Pyo, T.-S., Serabyn, E., Suto, H., Suzuki, R., Takato, N., Terada, H., Thalmann, C., Tomono, D., Turner, E. L., Watanabe, M., Yamada, T., Takami, H., Usuda, T., and Tamura, M.: 2013, *ApJ* **772**, 145
- Takami, M., Hasegawa, Y., Muto, T., Gu, P.-G., Dong, R., Karr, J. L., Hashimoto, J., Kusakabe, N., Chapillon, E., Tang, Y.-W., Itoh, Y., Carson, J., Follette, K. B., Mayama, S., Sitko, M., Janson, M., Grady, C. A., Kudo, T., Akiyama, E., Kwon, J., Takahashi, Y., Suenaga, T., Abe, L., Brandner, W., Brandt, T. D., Currie, T., Egner, S. E., Feldt, M., Guyon, O., Hayano, Y., Hayashi, M., Hayashi, S., Henning, T., Hodapp, K. W., Honda, M., Ishii, M., Iye, M., Kandori, R., Knapp, G. R., Kuzuhara, M., McElwain, M. W., Matsuo, T., Miyama, S., Morino, J.-I., Moro-Martin, A., Nishimura, T., Pyo, T.-S., Serabyn, E., Suto, H., Suzuki, R., Takami, M., Takato, N., Terada, H., Thalmann, C., Tomono, D., Turner, E. L., Watanabe, M., Yamada, T., Takami, H., Usuda, T., and Tamura, M.: 2014, *ApJ* **795**, 71
- Tamura, M., Gatley, I., Joyce, R. R., Ueno, M., Suto, H., and Sekiguchi, M.: 1991, *ApJ* **378**, 611
- Tamura, M.: 2009, in T. Usuda, M. Tamura, and M. Ishii (eds.), *American Institute of Physics Conference Series*, Vol. 1158 of *American Institute of Physics Conference Series*, pp 11–16
- Tanii, R., Itoh, Y., Kudo, T., Hioki, T., Oasa, Y., Gupta, R., Sen, A. K., Wisniewski, J. P., Muto, T., Grady, C. A., Hashimoto, J., Fukagawa, M., Mayama, S., Hornbeck, J., Sitko, M. L., Russell, R. W., Werren, C., Curé, M., Currie, T., Ohashi, N., Okamoto, Y., Momose, M., Honda, M., Inutsuka, S.-i., Takeuchi, T., Dong, R., Abe, L., Brandner, W., Brandt, T. D., Carson, J., Egner, S. E., Feldt, M., Fukue, T., Goto, M., Guyon, O., Hayano, Y., Hayashi, M., Hayashi, S. S., Henning, T., Hodapp, K. W., Ishii, M., Iye, M., Janson, M., Kandori, R., Knapp, G. R., Kusakabe, N., Kuzuhara, M., Matsuo, T., McElwain, M. W., Miyama, S., Morino, J.-i., Moro-Martin, A., Nishimura, T., Pyo, T.-S., Serabyn, E., Suto, H., Suzuki, R., Takami, M., Takato, N., Terada, H., Thalmann, C., Tomono, D., Turner, E. L., Watanabe, M., Yamada, T., Takami, H., Usuda, T., and Tamura, M.: 2012, *PASJ* **64**, 124
- Whitney, B. A., Wood, K., Bjorkman, J. E., and Cohen, M.: 2003, *ApJ* **598**, 1079

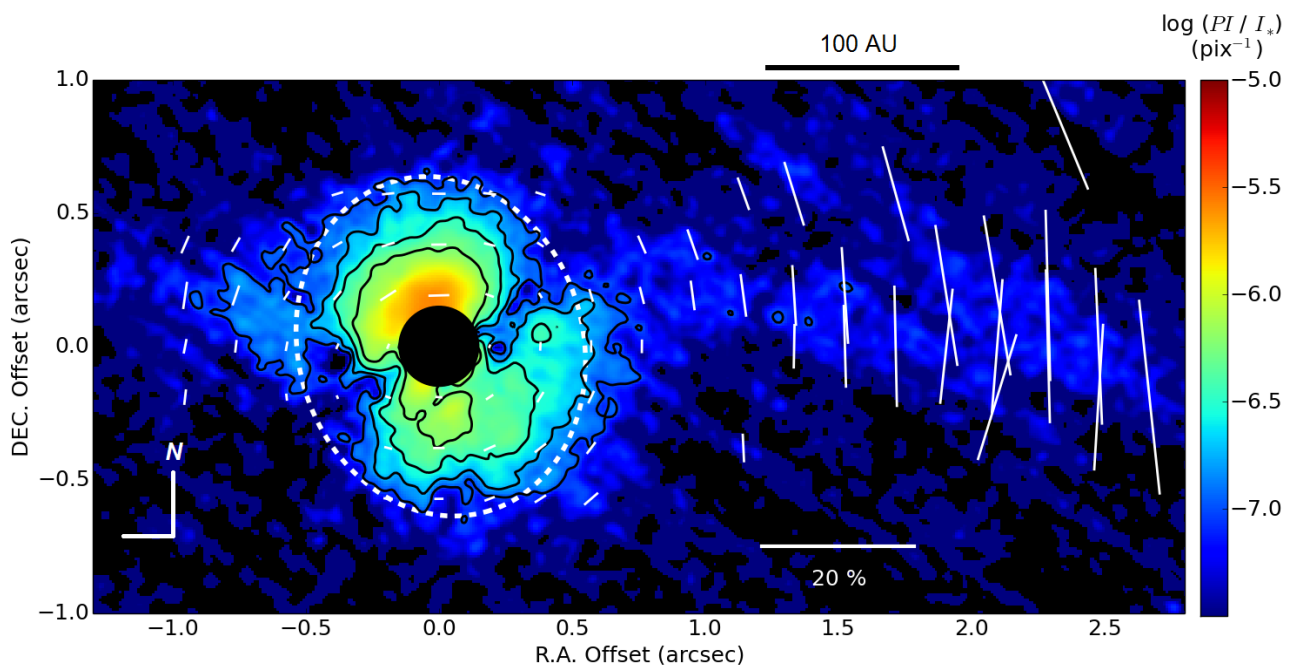


Fig. 1.— PI image of SU Aur in log-scale overlaid with polarization vector map. The PI flux at each pixel is scaled by the spatially integrated stellar I flux ($PI/I_* = 10^{-7}$ corresponds to $2.8 \text{ mJy arcsec}^{-2}$). The contours are shown for a log scale of PI/I_* of -7.0 , -6.75 , -6.5 and -6.25 . The dotted white ellipse is adjusted to the outermost contour (see text for details). The region within $r = 0''.15$ ($\sim 20 \text{ AU}$) is masked to show only regions where the measurements are reliable.

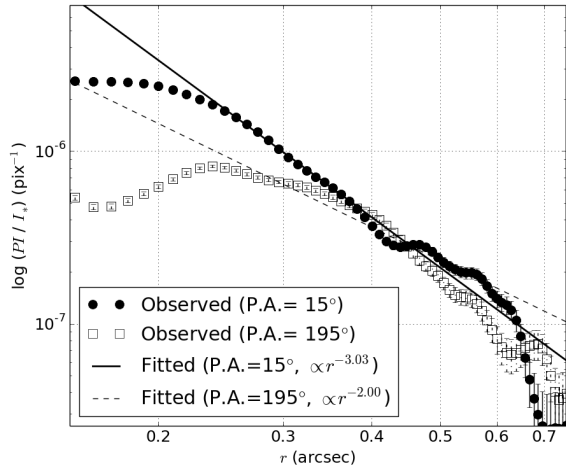


Fig. 2.— Radial PI/I_* profiles along the semi-major axis of the disk. The filled circles and solid squares show the measured value at P.A.s of 15° and 195° , respectively. The solid and dashed lines show power-law fits made at $r=0''.25-0''.6$, where r is the projected distance to the star.

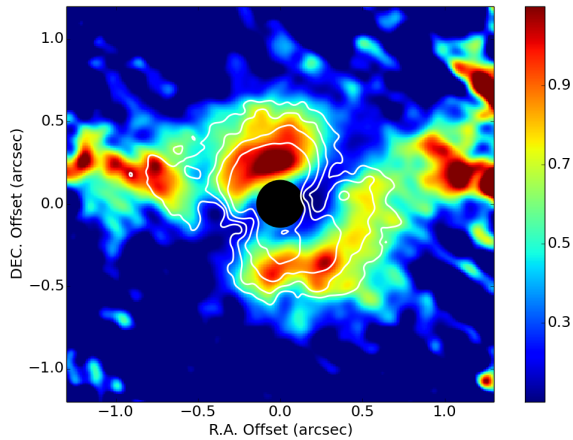


Fig. 3.— The outer disk and tails, highlighted by scaling the PI flux at each pixel by R^2 , where R is the projected distance to the star. The image is shown within $1''.3$ of the star, where this image processing does not significantly enhance background fluctuation. The color scale is arbitrary. The white contours show the original PI flux distribution shown in Figure 1.

Table 1: Parameters for SU Aur

Parameter		Reference
Spectral Type	G2III	1
Stellar Mass	$1.9 \pm 0.1 M_{\odot}$	2
Age	6.8 ± 0.1 Myr	2
Dust mass of the disk	$1-3 \times 10^{-4} M_{\odot}$	3
Mass accretion rate	$0.5-3 \times 10^{-8} M_{\odot} \text{ yr}^{-1}$	4,5
Distance	143^{+17}_{-13} pc	6
A_V	0.9 mag	2
H mag.	6.56 mag	7

References. — [1] Herbig (1952) ; [2] Bertout et al. (2007) ; [3] Ricci et al. (2010); [4] Calvet et al. (2004); [5] Ricci et al. (2010); [6] Bertout and Genova (2006); [7] 2MASS All Sky Catalog of Point Sources

Table 2: LOCI Parameters

Parameter ^a	Values ^b
N_A	$150 \times \text{FWHM}$
dr	$5 \times \text{FWHM}$ ($r < 50 \times \text{FWHM}$) $100 \times \text{FWHM}$ ($r > 50 \times \text{FWHM}$)
g	1
N_{σ}	$0.1/0.3/0.5/1.0 \times \text{FWHM}$

^a N_A ... the size of the optimization area; dr ... the width of the subtraction area; g ... the ratio of radial and azimuthal width for the optimization area; N_{σ} ... the minimum displacement distance in the azimuthal direction (Lafrenière et al. 2007).

^bFWMH is that of the observations (0'08).